

Development of a 3-Year-Old Child FE Head Model, Continuously Scalable from 1.5- to 6- Year-Old

Chiara Giordano, Svein Kleiven

Abstract This study summarised efforts in developing a 3-year-old FE head model, continuously scalable in the range 1.5- to 6-year-old. The FE models were transformed into one another using nonlinear scaling driven by control points corresponding to anthropometric dimensions. Procedures to mimic age-specific structural changes occurring during the paediatric development were implemented by means of transition of elements. The performances of the head models were verified on drop and compressive tests available from the literature. A stable and experimentally well-correlated family of FE models in the range 1.5- to 6-year-old was created.

Keywords child head, child modeling, finite element analysis, morphology, scaling procedure

I. INTRODUCTION

The introduction of child restraint systems has led to an improvement of the protection of children in motor vehicle crashes. However, still 32% of European road traffic fatalities involve children car occupants up to 14 years of age [1] and car crashes remain the second leading cause of death for children between 5 and 14 years old (y.o.) [2]. Independent of the crash direction, for forward-facing children, the most frequent injuries occur in the head including fractures to the skull, face, cerebral contusions and intracranial haemorrhage [3]. According to [4], the main cause of injury is contact with the car interior, such as an impact to the back of the front seat, the door panel or the windows.

To reduce the occurrence of head injuries, a thorough understanding of paediatric biomechanics is necessary. Traditionally, impact injury rating is evaluated by crash tests involving Anthropometric Test Devices (ATDs). For children Hybrid III, CRABI, P series and Q series are available on the market covering a range from 0 to 10 y.o. anatomy. ATDs are mechanical analogs that aim to replicate human behaviour under comparable loading conditions (i.e., comparable deformations, accelerations, articulations of the body regions, and similar interactions with seats and restraints). However, many studies question the biofidelity of dummies and their ability to provide detailed injury responses [5-7]. Because of simplifications and limitations arising from the need of a physical implementation, dummies are typically designed to match regulation requirements (R44, R129 in Europe) and they do not attempt to represent accurately the human anatomy and its evolution with age, not even at regional level. Moreover, in virtual absence of relevant Post Mortem Human Subjects (PMHSs) data, performance requirements have been set by using simplified scaling assumptions [8] and have been mostly limited to kinematic behaviours.

Human Body Models (HBMs), in particular Finite Element (FE) models, have the potential to accurately represent the anatomically complex geometry and topology of the human head and its development with age. They indeed combine anatomical and material detail, allowing inhomogeneous, anisotropic and nonlinear biological-like materials to be simulated. The use of a FE model enables assessment of local mechanical behaviour of the human body and it is of special interest for the head where relative skull-brain motion or brain deformation can be measured and successively used to estimate human tolerances to external forces (head injury risk curves). Unlike dummies, which are only available in few dimensions/ages (e.g. 50th percentile of the population), FE models can be implemented in multiple dimensions. HBMs therefore have the potential to better describe the diversity of children both in terms of anthropometry and biomechanical development. However, while great effort have been made to generate and validate detailed FE head models for adults [9-14],

fewer FE models for children have been presented in previous literature, involving many assumptions and scaling of properties from adult experiments [15-17]. Only in the last a few years, more anatomically detailed models have started being generated [18-19].

The development of a child FE head model faces numerous challenges. As first, the paediatric head cannot be modelled as a miniature adult head [20-21]. Significant age-related differences in brain and skull mechanical properties were found in many studies [22-24], indicating that computer models incorporating age-specific data are necessary to accurately mimic the paediatric response to impact. The brain and skull are subjected to a maturational process that takes place before birth and continues until adolescence in a relatively unrelenting way [25]. In the brain, changes appear in cortical folding, involution of the germinal layer and myelination within white matter. Lateral ventricles and white matter tracks significantly increase past the age of 4 y.o., while grey matter significantly decreases [26-27]. The brain water content decreases from 88% at birth to 80% at 1.5 y.o., and 78% at adult age. These anatomical attributes are important for understanding material property changes of the brain with age. In the skull, changes are mainly due to ossification processes [28-29]. At birth the skull consists of five bones separated by fibrous joints (sutures) and fibrous membranes (fontanelles), which allow movement that facilitates childbirth and brain growth throughout infancy and childhood. While the edges of many bone plates join together in early childhood, they do not become completely fused until adulthood [28]. Softer structures in the skull allow broader movements, making the cranial bone partially compressible and capable of slightly changing shape. From a mechanical point of view sutures and fontanelles exhibit a different behaviour with respect to the skull bone and they must be considered in FE child head modelling.

The aim of this study was to develop and validate a 3 y.o. FE head model continuously scalable in the range 1.5 to 6 y.o. (and perhaps beyond). The model and its scaled versions were developed in order to capture age-specific anatomical and functional changes occurring during the paediatric development. Global geometrical changes, such as variation in proportions between the upper and lower part of the face, are obtained by Kriging scaling [30] using the PIPER Kriging tool. Structural changes such as the replacement of growth cartilage by bone or the development of white matter tracts were implemented by the means of a transition of elements in the model (see Methods). Finally, age-specific material properties were assigned to the models [31] in order to capture the age-dependent mechanical response of biological tissues. The development and validation of these models is part of the efforts of the European PIPER project. During the course of PIPER project the head model will be integrated in a full body human body FE model for various safety applications. These may include investigation of full body model response in frontal and side impacts. The possibility of future investigations of injury mechanisms is also open.

II. METHODS

The Baseline Model

Geometry and Components of the Model In this study a FE model of a 3 y.o. child head, continuously scalable in the range 1.5-y.o., was developed in LS-DYNA code. The baseline model (3 y.o.) was based on computer tomography and medical imaging of one child provided by the Hospices Civils de Lyon (HCL, France). The segmentation of the images was performed by Ifsttar, partner of the European PIPER project, under a legal agreement allowing the communication of anonymized imaging dataset to help build human numerical models for safety. The 3 y.o. model consists of 14,999 nodes, 30,389 solid elements and 7,565 shell elements (Figure 1). It includes the scalp, the skull (two cortical layers of bone and the diploe), the cerebrum, cerebellum, meninges, falx, tentorium and the cerebrospinal fluid. Sutures of the skull and fontanelles were modelled as cartilaginous deformable tissue. Separate representation of grey and white matter was also implemented, as potentially important in head injury analysis. The volume ratio of white matter to grey matter was chosen to be equal to 0.44 according to data from [32]. Parametrical choices concerning the anatomy of the head were based on Generator of Body Data (GEBOD) anthropometric database [33] and are reported in Table I. The total mass of the head model is 2.7 Kg. A Kriging scaling procedure was adopted to scale the patient-specific model in order to obtain dimensions close to the average of the 3 y.o. group (Table I). In agreement with statistical data in [34], the skull thickness is location-dependent and varies between 3.45 mm in the parietal region to 5.79 mm in the occipital region.

The multi-block approach available in ANSYS ICEM 15.0 (ANSYS, Canonsburg, PA, USA) was used to mesh solid and shell elements. The inner and the outer layer compact bone of the skull were modelled by shell elements; the diploe layer of the cranium, cerebrum, cerebellum and the cerebrospinal fluid were represented by solid elements. Finally, the dura mater, tentorium and the falx were modelled by membrane elements. A typical spatial resolution of 3–5 mm was chosen to capture fundamental anatomical structures but, at the same time, reduce the computational cost of the simulations. The aim of the model is indeed to be robust and scalable, without altering the mesh quality. The element quality of the 3 y.o. head model is listed in Table II.

TABLE I
PARAMETRICAL CHOICES CONCERNING THE ANATOMY OF THE 50TH PERCENTILE 3 Y.O. HEAD [31]

<i>Head Circumference</i>	cm	50.2
<i>Head Length</i>	cm	17.5
<i>Head Breadth</i>	cm	13.7
<i>Lower Face Height</i>	cm	8.5
<i>Face Height</i>	cm	14.7
<i>Head Height</i>	cm	17.9
<i>Tragion to Top of Head</i>	cm	11.7

TABLE II
3D ELEMENT QUALITY OF THE 3-YEAR-OLD CHILD HEAD MODEL

Quality Name	Min or Max Value	Allowable	Violated
<i>Jacobian</i>	0.1	> 0.3	(217/30389) 1%
<i>Min side Length</i>	0.2 mm	> 1 mm	(1015/30389) 3%
<i>Aspect Ratio</i>	16.85	< 8	(224/30389) 1%
<i>Warpage</i>	79.24°	< 50°	(84/30389) 0%
<i>Min quad Angle</i>	5.81°	> 15°	(39/30389) 0%
<i>Max Quad Angle</i>	176.65°	< 165°	(58/30389) 0%

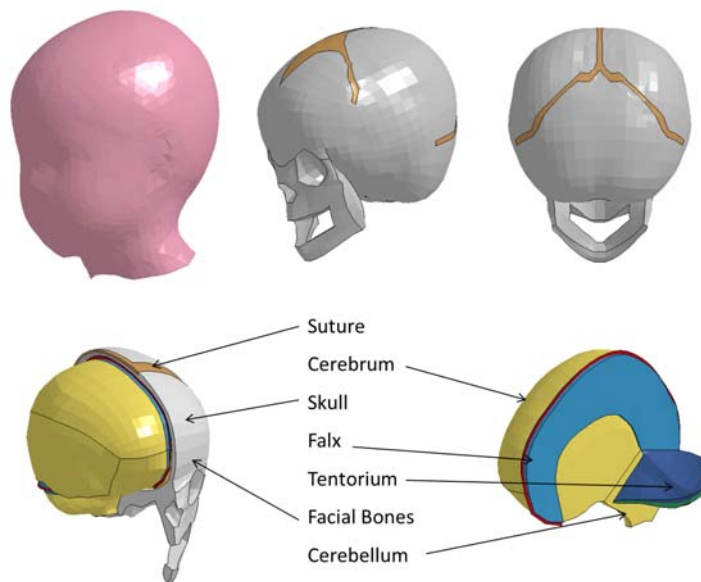


Fig. 1 - The baseline head model. On the top the isometric view of the head model is presented (scalp in pink, skull in grey, sutures in brown). On the bottom, the brain is exposed to show the inner membranes and brain components.

Material Properties A summary of the material properties for the 3 y.o. head model is reported in Table III. Due to ethical reasons, there is paucity in experimental data concerning the mechanical properties of the child

head; therefore, interpolation or scaling procedures from adult data are sometimes needed.

Material properties for brain tissue were based on experimental evidence from [22] [35-36]. In [22] a significant variation of porcine brain shear modulus was found between infants (5 porcine days ~ 1 human month) and children (4 porcine weeks ~ one–three human years). However, no statistical significant variation was observed between child and adult specimens. In [35] test results on rat brain samples showed statistically indistinguishable brain shear moduli for 43 day-old samples (3 human years) and 90 day-old samples (6 human years). Human data from [36] confirmed significant difference between the infant (2-5 month-old) and the toddler (2 y.o.) brain shear modulus but, again, no statistical difference in brain shear modulus was found between 2 y.o. and 50 y.o. brain samples. This experimental evidence suggested that the age-dependent material properties of brain tissue change rapidly during the first couple of years of life and more gradually later in the childhood. For this reason, the 3 y.o. brain tissue has been considered equivalent to adult tissue and data from [13] for an adult FE head model were used. Brain tissue was modelled as a nonlinear viscoelastic model described by an Ogden 2nd order constitutive law with $\alpha_1 = 10.1$, $\alpha_2 = -12.9$, $\mu_1 = 53.8$ Pa and $\mu_2 = -120.4$ Pa. Viscosity was added by means of 6 modes identified on brain tissue relation experiments [13].

Material properties for dura mater were chosen based on studies by [37-38]. In these studies the authors performed axisymmetric biaxial tension at 0.02 mm/s on paediatric dural tissue and reported dura mater mechanical behaviour to be best characterised by a nonlinear elastic constitutive model. In the current study, a Mooney-Rivlin constitutive law was chosen to represent the nonlinear elastic behavior of the dura mater.

To the best knowledge of the authors, no experimental data on paediatric human or animal pia mater is currently available in the literature. However, [39-40] published data on bovine pia-arachnoid complex, reporting isotropic linear elastic behaviour of the membrane before failure. Given the lack of information about paediatric material characteristics, adult material properties were used for the pia mater in the FE model. A linear elastic constitutive law was assigned to pia mater elements with a Young Modulus of 11.5 MPa and a Poisson ratio of 0.45. It is however unknown if these characteristics are applicable to the paediatric brain.

The cerebrospinal fluid (CSF) was modelled with material properties similar to water, based on a study by [41]. In this study, samples of human CSF were collected from patients from age 1 month to 69 y.o. and tested using a rheometer. All specimens exhibited a viscosity similar to water and the behaviour of CSF was found to be age-independent (infant viscosity 0.727 mPa·s, 17 y.o. viscosity 0.748 mPa·s, 73 y.o. viscosity 0.735 mPa·s). An elastic fluid constitutive law was therefore used in the FE model with a bulk modulus of 2.1 GPa.

Material properties for skull bone were obtained by interpolation from experimental data by [24] [42-44]. To the best knowledge of the authors, the mechanical properties of 3 y.o. skull bone remain undocumented. However, it was possible to use data from the literature to identify a mathematical model able to describe the

TABLE III
SUMMARY OF THE PROPERTIES OF THE 3 Y.O. HEAD MODEL COMPONENTS USED IN THIS STUDY. THE CAPITAL LETTER K REPRESENTS THE BULK MODULUS.

Tissue	Young's Modulus	Density [Kg/dm ³]	Poisson's Ratio
<i>Scalp</i>	Ogden 1st order + viscosity [44]	1.14	0.49
<i>Outer Compact Bone</i>	4.6 GPa	2.00	0.22
<i>Inner Compact Bone</i>	4.6 GPa	2.00	0.22
<i>Porous Bone</i>	1.0 GPa	1.30	0.24
<i>Suture</i>	8.1 MPa	1.50	0.22
<i>Brain Tissue</i>	Ogden 2nd order + viscosity [13]	1.04	~ 0.5
<i>Cerebrospinal Fluid</i>	K = 2.1 GPa	1.00	~ 0.5
<i>Dura Mater</i>	Mooney – Rivlin [36]	1.13	0.45
<i>Pia Mater</i>	11.5 MPa	1.13	0.45
<i>Falx</i>	31.5 MPa	1.13	0.45
<i>Tentorium</i>	31.5 MPa	1.13	0.45

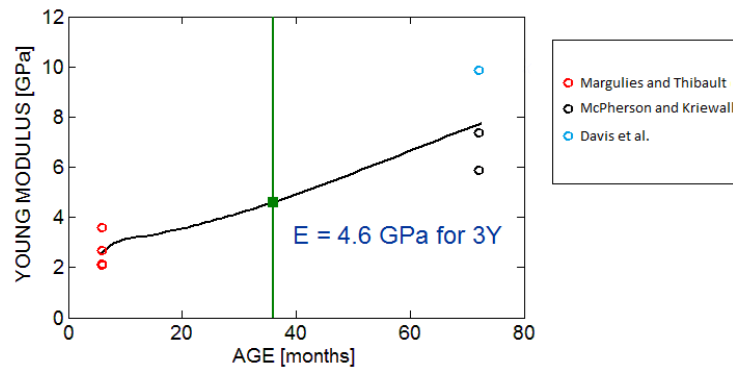


Fig. 2 - Cubic spline curve fit used to connect data on infant compact skull bone mechanics to the measured 6 y.o. elastic modulus [22], [40-42].

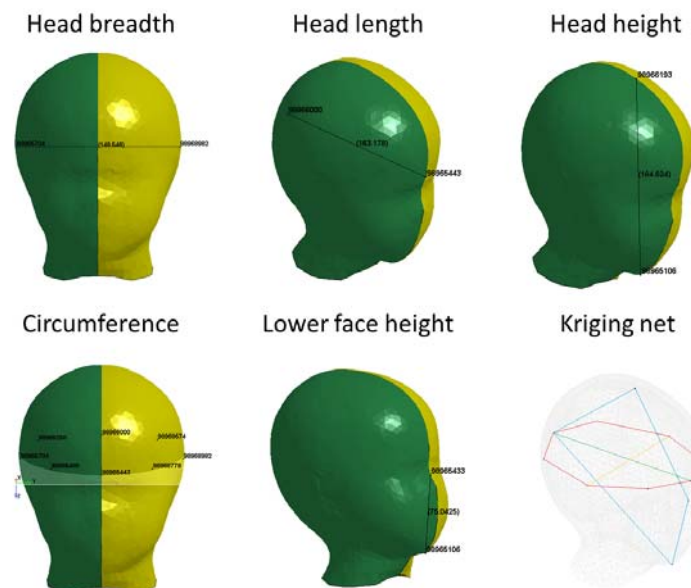


Fig. 3 - Points used to drive the Kriging transformation. Head length, head breadth, head height, circumference and lower face height are specified as targets to account for variation in head segments proportions with age.



Fig.4 - The 1.5 y.o (left) and 6 y.o models (right) obtained by scaling using the PIPER Kriging tool and the Kriging net reported in Figure 3. The head model has been attached to a new neck model developed as an effort in the PIPER European project (just for visualisation).

variation of skull bone mechanical properties with age according to data reported in the literature for other ages. Studies from [46] and [24] found an increase of elastic modulus and ultimate stress with donor age for infants. Recent data by [44] reported an average elasticity modulus of 9.87 GPa for 6 y.o. cranial cortical bone, indicating a positive correlation between skull stiffness and donor age even for older children. As previously done by [45], to estimate the elastic moduli in children between 1.5 and 6 y.o., a cubic spline curve fit can be used to connect data on infant skull bone mechanics to the measured 6 y.o. elastic modulus [24], [42-44]. Figure

2 represents the best empirical model identified from available data. From the curve fit, the elastic modulus for the compact bone of the skull for 3 y.o. child was estimated to be 4.6 GPa.

In the child FE head model, the cranial sutures were modelled with an isotropic linear elastic model characterised by a Young modulus of 8.1 MPa, based on experimental data by [24]. In this study, human paediatric cranial sutures were tested in tension at 1.20 and 2.38 m/s rates. The elastic modulus, ultimate stress and ultimate strain of the sutures were reported to be 8.1 ± 4.7 MPa, 4.7 ± 1.6 MPa and 1.5 ± 1.3 respectively. None of the material properties were affected by age or strain rate, giving the confidence to use this data to model 3 y.o. cranial sutures too.

The scaled models (1.5 y.o and 6 y.o)

The scaled models (1.5 and 6 y.o.) were obtained from the 3 y.o. baseline using the PIPER Kriging tool. The Kriging scaling technique allows accounting for global geometrical changes due to growth and requires the specification of a set of control points that define the location of specific nodes before and after the geometric transformation. Nonlinear least-squares estimation was performed, which calculates the unknown nodal displacements as a linear combination of the N known values (control points). Crucial for the performance of the method is a proper definition of the targets [30]. In the current study, the Kriging net was based on anatomical landmarks (glabella, opistocranium, tragus, vertex, nasion and mental protuberance) in order to account for variation in head segments proportions with age. Head length, head breadth, head height, circumference and lower face height (Figure 3) were specified as targets, according to data from GEBOD database [33]. The scaling error was in the range of ± 0.2 cm. The results of the Kriging transformation are reported in Figure 4.

As for the baseline model, separate representation of grey and white matter was implemented. According data from [32], the volume ratio of white matter to grey matter is age-dependent. For this in-vivo MRI study on healthy infants and children, the authors reported a fast white matter volume increase in the first 2 years of life while all major white matter fiber tracts could be identified by age 3 years. Consequently, for the 1.5 and 6 y.o. child FE model, the ratio of white matter to grey matter was adjusted to be 0.37 and 0.5 respectively. It is known that the development of white matter commences in the brain stem and progresses to the cerebellum and the cerebrum, generally proceeding from central to peripheral, from inferior to superior and from posterior to anterior [47]. The same pattern was followed to generate a transition of elements in the models between grey matter and white matter by implementing an algorithm that mimicked the growth of white matter tracts with priorities (Figure 5).

A transition of elements was also incorporated to take into account the ossification processes occurring in the skull between 6 months to 6 years old (Figure 6). According to data collected by [34], the cranial sutures

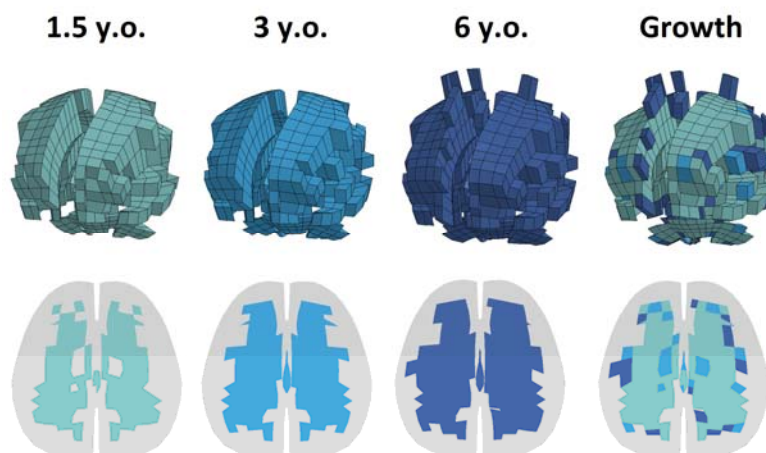


Fig. 5 - Results of the growth algorithm to adjust the ratio between white matter and grey matter with age. White matter tracts grow from central to peripheral (1), inferior to superior (2) and posterior to anterior (3). The centre of the growth is the brainstem.

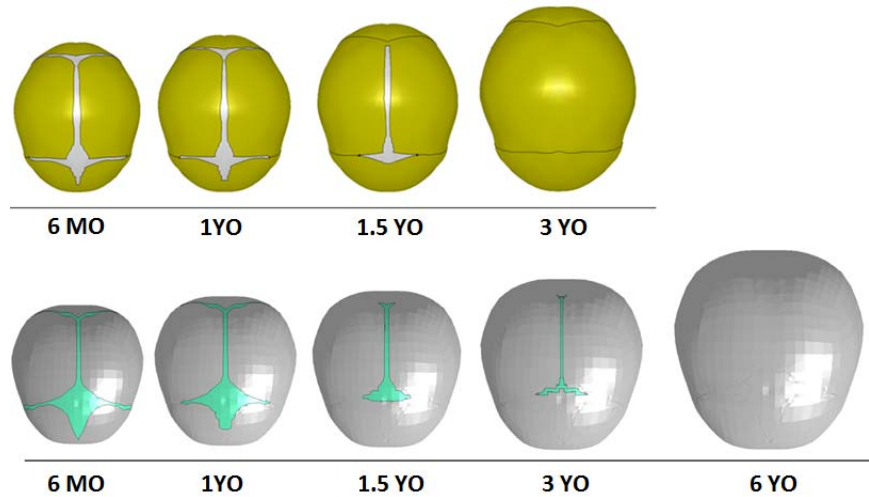


Fig. 6 – Transition of elements from the fibrous sutures to the bony skull to mimic the closure of the anterior fontanelle and cranial sutures. On the top, the statistical model by [32] is reported. On the bottom the family of FE head models is presented, from 6 months to 6 years of age.

gradually close from newborn to 6 years old. The suture closing speed is very different across the skull; in particular, the inferior region of lambdoid and coronal sutures and the region of the sagittal suture near the frontal cranium close more rapidly than other areas. In this study, the mesh of the anterior fontanelle and cranial sutures was based on computer tomography and medical imaging of one 6-month-old child. An ethical approval was granted from the ethical review board of Stockholm, Sweden (DNR 2011/1526-31/3) for the use of these images. Statistical data from [34] were used to implement the mechanism of closing of the sutures. Figure 6 represents the transition of elements between fibrous tissue (blue) to bone (brown), mimicking the closing of the sutures. The choice to generate the topology of the mesh from a younger age opens the possibility, in future, to scale the model down to younger ages. For the baseline model (3 y.o.), length and width of the cranial sutures were adjusted to match the CT images of the skull used to generate the model. The scaled 6 y.o. model has no fibrous sutures because the ossification process occurs mostly in the first two years from birth and, at 6 y.o., the cranial sutures are almost completely closed. Mechanically their effect is considered to be negligible.

A summary of the material properties for the scaled models is reported in Table IV and V. Due to paucity in experimental data, dura and pia mater were modelled with the same material properties used for the 3 y.o. model in both scaled models. In previous studies [24] [41], CSF and cranial sutures did not exhibit age-dependent behaviour. Therefore, in the scaled models, the same constitutive laws were used as in the baseline model. For the 6 y.o. child model, material properties for skull bone were taken from Davis et al. [44], while for the 1.5 y.o. child model they were interpolated from experimental data (Figure 3). From the curve fit, the elastic modulus of the skull was estimated to be 3.4 GPa. A linear isotropic elastic constitutive law was used to represent the behaviour of the skull. Finally, in the scaled models brain tissue was modelled as a nonlinear viscoelastic model described by an Ogden 2nd order constitutive law. According to previous studies [22][35-36], in the range 1.5 to 6 y.o., young brain tissue is considered equivalent to adult tissue.

Validation of the Head Model

Drop Tests The performances of the 1.5 and 6 y.o. head models were verified on non-destructive drop tests available from [48]. These tests were conducted to check the global properties of the head model (structural stiffness, kinematics and correct distribution of mass).

In Loyd's collection of experiments [48] the PMHS head was dropped from heights of 15 and 30 cm onto five different impact locations: vertex, occiput, forehead, left parietal, right parietal. For each drop, the head was placed into a fine net that was attached to a pulley using line. The head was then released by burning the fishing line, which allowed free fall to occur without rotation or out-of-plane-motion. The impact occurred with a smooth flat aluminum platen and the resultant acceleration of the head was measured.

In the simulations, the head model was subjected to gravity load (free fall) impacting a rigid aluminum plate.

The interface between the dura mater and the skull was modeled with tied-surface contacts in LS-Dyna. A *CONTACT_AUTOMATIC_SURFACE_TO_SURFACE card was used to simulate the impact between the head and the platen. The initial position of the model was determined from [48] in terms of drop height and impact angles with respect to the Frankfort and the horizontal plane (midsagittal impacts) or the right and left infraorbital foramen and the horizontal plane (lateral impacts). The resultant acceleration of the head was extracted from the simulations.

Compression Tests The performance of the 6 y.o. head model was also verified on compressive tests available from [48]. These tests were conducted to check the structural stiffness of the head model in the lateral direction. In the experiments, the PMHS head was placed between two aluminum platens. The parietal regions were in contact with the platens. The compression test battery consisted of a preconditioning test, one static deflection and three constant normalised displacement rate tests (0.01, 0.1, 0.3/s). Force-deflection curves were measured.

In this study, only the fast compression test (0.3/s) was simulated. The head model was positioned between two rigid aluminum platens and was subjected to compression by controlling the displacement of the top platen. The interface between the dura mater and the skull was modeled with tied-surface contacts while a *CONTACT_AUTOMATIC_SURFACE_TO_SURFACE card was used in LS-Dyna to simulate the contact between the platens and the head. The force-displacement curve was measured from the simulations.

III. RESULTS

Validation of the 6y.o. Head Model

The performances of the 6 y.o. head model were verified on drop tests available from [48]. Data referring to P18M (9 y.o.) was used as experimental target for the simulations. Figure 7 and Figure 8 show the initial positioning of the head model and the results of the simulations in terms of peak resultant acceleration and head resultant acceleration in time respectively. For all the tests, the model response was in agreement with the experimental data. The Normalized Integral Square Error (NISE) [49] was used as a quantitative evaluation to compare the predicted time history response with the measured data. Phase shift (N-phase), amplitude difference (N-amp), and shape difference (N-shape) were evaluated. The Error Measures (EMs) were then used to calculate a Correlation Score (CS). Detailed descriptions of the methods and equations used are presented in Appendix A. According to the biofidelity rating by [50], the CS values were categorized into five rating: excellent ($86 < CS < 100$), good ($65 < CS < 86$), fair ($44 < CS < 65$), marginal ($26 < CS < 44$), unacceptable ($0 < CS < 26$). The correlation scores for this study are reported in Table 6.

TABLE IV
SUMMARY OF THE PROPERTIES OF THE 1.5 Y.O. HEAD MODEL COMPONENTS USED IN THIS STUDY. THE CAPITAL LETTER K REPRESENTS THE BULK MODULUS.

Tissue	Young's Modulus	Density [Kg/dm ³]	Poisson's Ratio
Scalp	Ogden 1 st order + viscosity [44]	1.14	0.49
Outer Compact Bone	3.4 GPa	2.00	0.22
Inner Compact Bone	3.4 GPa	2.00	0.22
Porous Bone	1.0 GPa	1.30	0.24
Suture	8.1 MPa	1.50	0.22
Brain Tissue	Ogden 2 nd order + viscosity [13]	1.04	~ 0.5
Cerebrospinal Fluid	K = 2.1 GPa	1.00	~ 0.5
Dura Mater	Mooney – Rivlin [36]	1.13	0.45
Pia Mater	11.5 MPa	1.13	0.45
Falx	31.5 MPa	1.13	0.45
Tentorium	31.5 MPa	1.13	0.45

TABLE V
SUMMARY OF THE PROPERTIES OF THE 6 Y.O. HEAD MODEL COMPONENTS USED IN THIS STUDY. THE CAPITAL LETTER K REPRESENTS

THE BULK MODULUS.

Tissue	Young's Modulus	Density [Kg/dm ³]	Poisson's Ratio
<i>Scalp</i>	Ogden 1 st order + viscosity [44]	1.14	0.49
<i>Outer Compact Bone</i>	9.0 GPa	2.00	0.22
<i>Inner Compact Bone</i>	9.0 GPa	2.00	0.22
<i>Porous Bone</i>	1.0 GPa	1.30	0.24
<i>Brain Tissue</i>	Ogden 2 nd order + viscosity [13]	1.04	~ 0.5
<i>Cerebrospinal Fluid</i>	K = 2.1 GPa	1.00	~ 0.5
<i>Dura Mater</i>	Mooney – Rivlin [36]	1.13	0.45
<i>Pia Mater</i>	11.5 MPa	1.13	0.45
<i>Falx</i>	31.5 MPa	1.13	0.45
<i>Tentorium</i>	31.5 MPa	1.13	0.45

Further validation of the 6 y.o. head model is provided in terms of model response to low-rate compression [48]. Once again, data referring to P18M (9 y.o.) was used as experimental target for the simulations. Figure 9 shows the initial positioning of the head model and the results of the simulations in terms force-deflection curves. For this test, the model response was in agreement with the experimental data. The correlation scores are reported in Table 6 together with the biofidelity rating.

Validation of the 1.5 y.o. Head Model

The performances of the 1.5 y.o. head model were verified in drop tests available from [48]. Data referring to P17F (1.8 y.o.) was used as experimental target for the simulations. In the [48] report the evolution of the average acceleration in time is unfortunately missing but pulse duration and peak acceleration of the experimental curves are reported. Figure 10 shows the initial positioning of the head model and the comparison between the pulse durations and acceleration peaks. For all the tests, the kinematics of the impact and the model response were in agreement with the experimental data. The NISE analysis could not be performed because of missing time history data.

IV. DISCUSSION

This study summarised efforts in developing a 3 y.o. FE head model, continuously scalable in the range 1.5 to 6 y.o. The FE models were transformed into one another using nonlinear scaling driven by control points

TABLE VI
SUMMARY OF THE PERFORMANCES OF THE 6 Y.O. HEAD MODEL (NISE [47-48]). MORE DETAILS CAN BE FOUND IN APPENDIX A

Test	CS Phase	CS Amplitude	CS Shape	Biofidelity
<i>Left Parietal 15</i>	99.96542	99.63330	96.85724	Excellent
<i>Left Parietal 30</i>	98.71136	99.93425	98.81990	Excellent
<i>Right Parietal 15</i>	97.50744	99.97192	97.77376	Excellent
<i>Right Parietal 30</i>	98.02463	99.86397	98.50979	Excellent
<i>Occiput 15</i>	98.65623	99.86640	98.99562	Excellent
<i>Occiput 30</i>	97.60964	99.88626	97.70944	Excellent
<i>Vertex 15</i>	97.87419	99.86548	98.06549	Excellent
<i>Vertex 30</i>	98.44660	99.83410	99.65979	Excellent
<i>Forehead 15</i>	97.88925	99.89003	99.82870	Excellent
<i>Forehead 30</i>	99.69836	99.46896	96.96609	Excellent
<i>Compression 0.3/s</i>	94.30347	99.91364	93.98368	Excellent

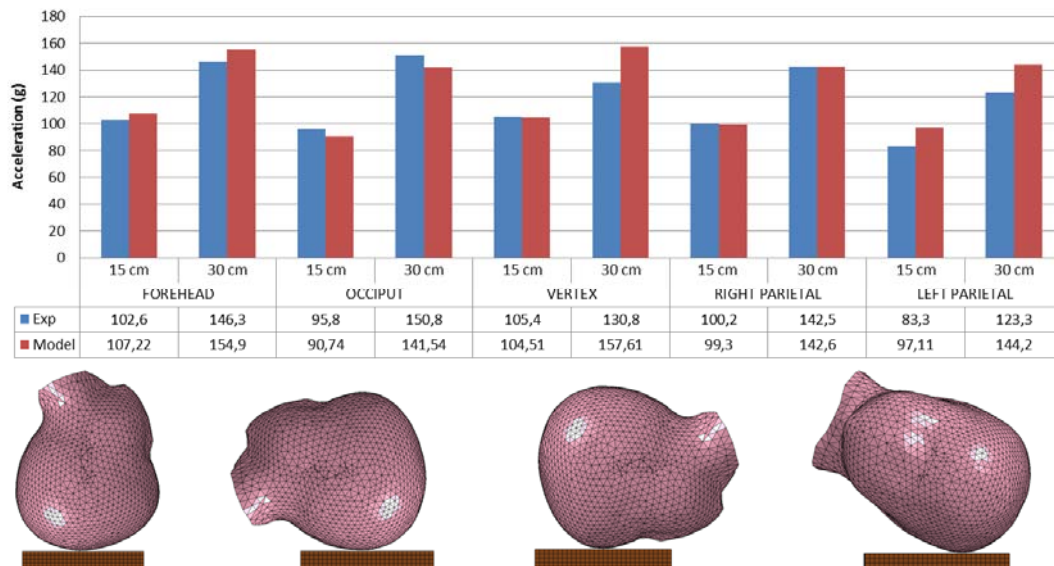


Fig. 7 – On the top: summary of the drop test results for all the impact locations. Peaks of acceleration are reported for both experimental data (blue) and simulated curves (red). On the bottom: set-up of the drop tests. The head was dropped from a height of 15 and 30 cm to an aluminum plate onto five locations.

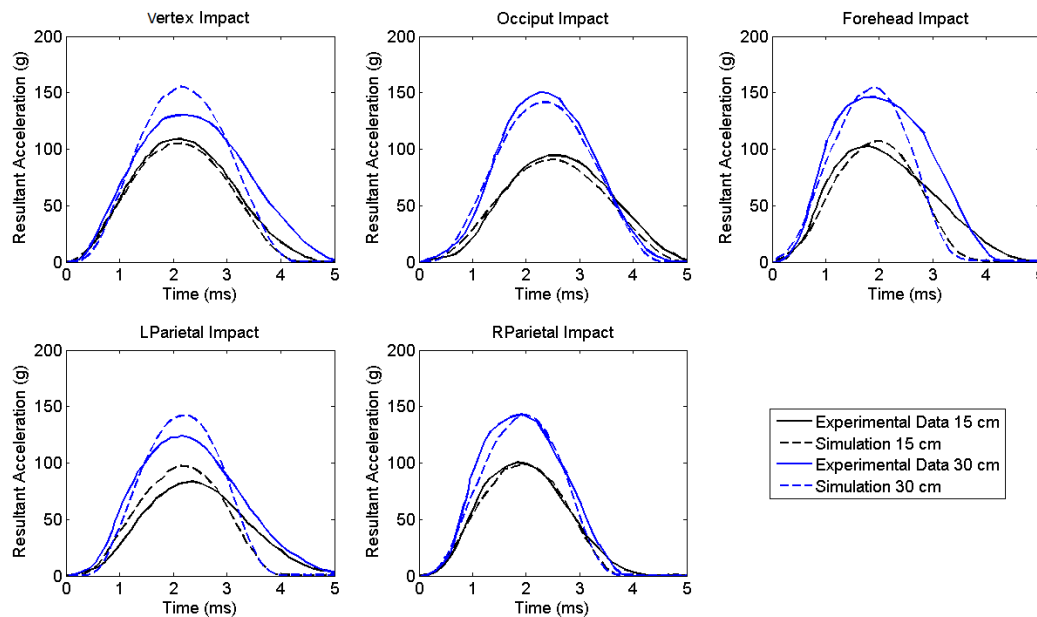


Fig. 8 - Comparison of experimental and simulated acceleration curves for all the tests. Experimental results are reported in full line while simulated curves are in dashed line.

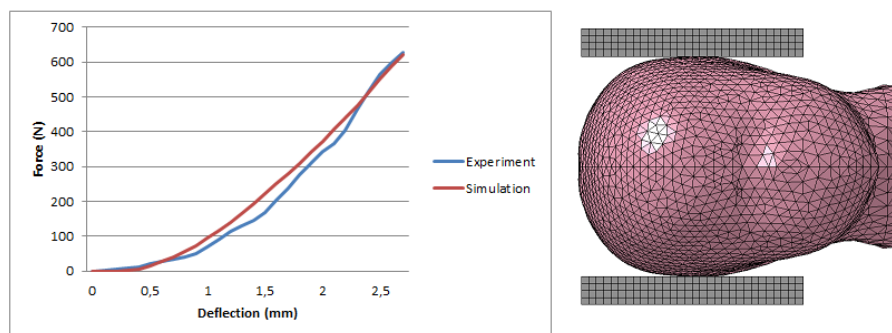


Fig. 9 - Comparison of experimental and simulated force-deflection curves for the compression test (0.3/s). Experimental results are reported in blue while simulated curves are in red.

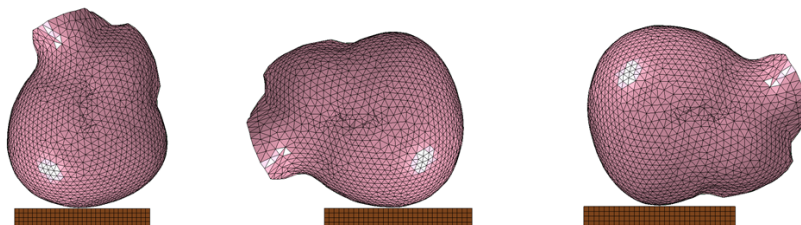
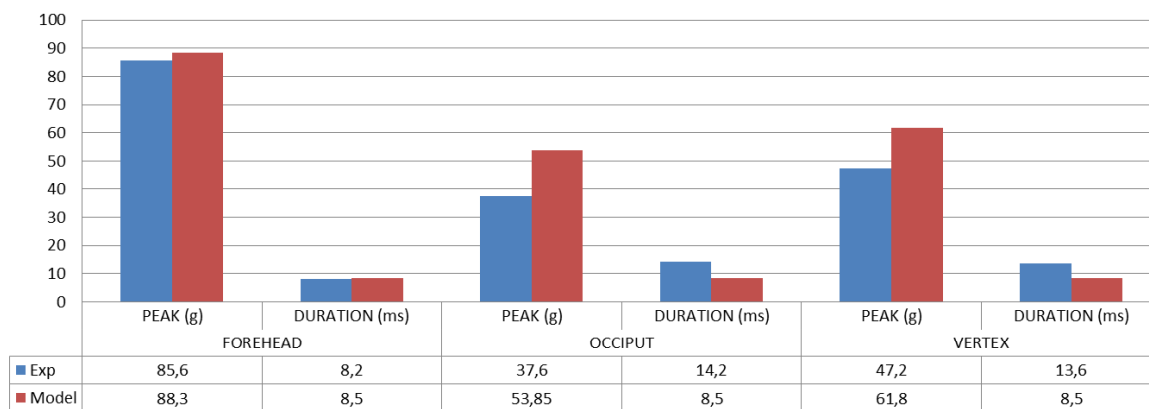


Fig. 10 – On the top: summary of the drop test results for all the impact locations. Peaks of acceleration are reported for both experimental data (blue) and simulated curves (red) together with the duration of the impact. On the bottom: set-up of the drop tests. The head was dropped from a height of 15 to an aluminum plate onto three locations.

corresponding to anthropometric dimensions. The scaling approach was automated (PIPER European project) and models corresponding to any age target could be generated within this range. Thanks to the integration of open anterior fontanel and sutures of the skull in the mesh, extrapolation outside this range can also be considered (6 months to 10 y.o.). Procedures to mimic age-specific anatomical and functional changes occurring during the paediatric development were implemented. Structural changes, such as the replacement of growth cartilage by bone or the development of white matter tracts, were generated by means of transition of elements in the model. To the best knowledge of the authors, this is the first time that such a family of FE models has been developed. The modelling effort was funded by the European Commission F7 – PIPER project (more details can be found at www.piper-project.eu) and the FE models will be made available Open Source under a GPL v3 license with Open Science clauses after the end of the project (April 2017).

When possible, age-specific material properties were assigned to the FE models [31] in order to capture the age-dependent mechanical response of biological tissues. Due to scarcity of paediatric PMHS data, interpolation or scaling procedures from adult data were sometimes needed. These assumptions represent the biggest limitation of the finite element analysis. Adult material properties were indeed used in the model for the membranes and the scalp while interpolated properties were used for the skull. It is however debatable if these characteristics are applicable to the paediatric head.

Due to the lack of experimental data concerning paediatric injury biomechanics, the validation of the model was challenging. For this family of models, non-destructive drop tests available from [48] were used to check the global properties of the head model, such as the model structural stiffness, kinematics and internal distribution of masses. The 6 y.o. model was compared to experimental data from a 9 y.o. cadaver while the 1.5 y.o. model is compared to experimental data from a 1 y.o + 10 months. It is of course not optimal to have non-matching ages for experiments and models; however, the dimensions and the dropped masses of the PMHSs were comparable to the models. In absence of other relevant data, this solution has been assumed to be acceptable. The 6 y.o. FE model shows mostly excellent/good performances for this data set. For all the tests, the kinematics of the impact and the model response are in agreement with the experimental data. An exception occurs for the left parietal impact where the simulated average acceleration is higher than the experimental. It is however interesting to notice that the FE model, because of construction, replies symmetrically during the left and right parietal impacts (peak acceleration R15 = 99 g, L15 = 97 g, R30 = 143 g,

L30 = 144 g) while the PMHS head shows asymmetry in the experimental results (peak acceleration R15 = 100 g, L15 = 83 g, R30 = 142 g, L30 = 123 g). The 1.5 y.o. FE model shows fair/good performance for this data set. For all the tests, the characteristics of the impact are plausible but the simulated average acceleration tends to be higher than the experimental and the impact duration shorter. Moreover, partial data only is available for the 1.8 y.o. subject (PM17F), making the analysis more difficult. In the [48] study the PMHS head was only impacted from 15 cm onto the forehead, occiput and vertex. During the 15 cm vertex impact the PMHS head sustained indeed a diastatic linear fracture of the left coronal suture. A CT scan of the fracture showed that it extended across the length of the left coronal suture and no more tests were performed on the same subject. The presence of the fracture could explain the huge difference (> 50%) in peak magnitude and curve duration between the forehead impact and the occiput and vertex impacts (experimental). For the forehead impact, when the skull was supposedly intact, the FE model was indeed able to reproduce the experimental curve.

The performances of the 6 y.o. head model were also verified on compressive tests available from [48]. These tests were conducted to check the structural stiffness of the head model in the lateral direction. Unfortunately, this data is not available for PM17F (1.8 y.o.). The compression test battery consisted of a preconditioning test, one static deflection and three constant normalised displacement rate tests (0.01, 0.1, 0.3/s). In this study, due to numerical challenges in simulating low-rate compression with LS-DYNA explicit solver (time step), only the fastest compression test (0.3/s) was simulated (1 second was simulated in approximately 200 hours). The kinematics of the impact is plausible and the model response is in agreement with the experimental data, showing a correct global stiffness of the 6 y.o. head.

For future studies, it is important to expand the validation matrix. A reliable FE model should be able to reproduce the local response (stress, strain) of several experimental settings for the intended use and the benchmark testes should include a broad range of possible impacts. However, for the time being, given the lack of experimental data, the validation of a child model cannot be performed against cadaver experiments in the same way as in adult head. One alternative way could be scaling adult cadaver experimental data of relative skull-brain motion in order to study the local skull-brain response of the model [51]. This kind of data is not available for children but it would be of great interest for studying the capability of the models in predicting traumatic brain injuries. Once the validation is completed, these FE models could become an important tool for investigating the biomechanical response of the human body in crash scenarios, which in turn could help the development or optimization of safety systems to prevent injury.

V. CONCLUSIONS

Scaling methods with adjusting procedures can be used to obtain a stable and experimentally well-correlated family of FE models in the range 1.5 to 6 y.o. Global geometrical changes were obtained by scaling driven by control points corresponding to anthropometric dimensions. Structural changes (growth) were implemented by means of transition of elements in the model. Age-specific material properties capture the age-dependent mechanical response of biological tissues. The scaled models show good performances in reproducing non-destructive drop tests and lateral compressive tests. Once the validation is completed, this family of models has the potential to be an important tool for optimisation of child safety systems.

VI. ACKNOWLEDGEMENT

This research has received funding from the European Union Seventh Framework Programme (PIPER project). Dr. Phippe Beillas (Ifsttar-UCBL) is greatly acknowledged for the provision of the segmentation data, which this paper is based on. This contribution was fundamental for the study. The Hospices Civils de Lyon (Lyon, France) is acknowledged for providing the 3 y.o. anonymized CT-scan to Ifsttar.

VII. REFERENCES

- [1] Peden M, Oyegbite K et al. World Report on Child Injury Prevention. World Health Organization, Geneva, Switzerland, 2008.
- [2] Peden M, Toroyan T, Harvey A, Bartolomeos K, Iaych K. Global Status Report on Road Safety: Time for Action, World Health Organization, Geneva, Switzerland, 2009.

- [3] Arbogast KB, Chen I, Durbin DR, Winston FK. Injury risks for children in child restraint systems in side impact crashes. *Proceedings of IRCOBI Conference*, 2004, Graz, Austria.
- [4] Bohman K, Arbogast KB, Bostrom O. Head injury causation scenarios for belted, rear-seated children in frontal impact. *Traffic Injury Prevention*, 2001, 12: 62–70.
- [5] Seacrist T, Locey CM, Mathews EA, Jones DL, Balasubramanian S, Maltese MR, Arbogast KB. Evaluation of pediatric ATD biofidelity as compared to child volunteers in low-speed far-side oblique and lateral impacts. *Traffic Injury Prevention*, 2014, 15, Suppl 1:S206-14.
- [6] Wu J, Cao L, Reed MR, Hu J. A simulation study of spine biofidelity in the hybrid-III 6-year-old ATD. *Traffic Injury Prevention*, 2013, 14: 397-404.
- [7] Shaw CG, Crandall JR, Butcher J. Biofidelity Evaluation of the THOR Advanced Frontal Crash Test Dummy. *Proceedings of IRCOBI Conference*, 2000, Montpellier, France.
- [8] Irwin AL, Mertz HJ, Elhagediab AM, Moss S. Guidelines for Assessing the Biofidelity of Side Impact Dummies of Various Sizes and Ages. *Stapp Car Crash Journal*, 2002, Vol. 46, P-383.
- [9] Zhang L, Yang KH, King AI. A proposed injury threshold for mild traumatic brain injury. *Journal of Biomechanical Engineering*, 2004, 126:226-236.
- [10] Willinger R, Baumgartner D. Human head tolerance limits to specific injury mechanisms. *International Journal of Crashworthiness*, 2003, 8: 605-616.
- [11] Horgan T, Gilchrist MD. The creation of three-dimensional finite element model for simulating head impact biomechanics. *International Journal of Crashworthiness*, 2003, 8: 353-366.
- [12] Takhouas EG, Eppinger RH, Campbell JQ, Tannous RE, Power ED, Shook LS. On the Development of the SIMon Finite Element Head Model. *Stapp Car Crash Journal*, 2003, 47: 107-133.
- [13] Kleiven S. Predictors for traumatic brain injuries evaluated through accident reconstructions. *Stapp Car Crash Journal*, 2007, 51: 81-114.
- [14] Ji S, Zhao W, Ford JC et al. Group-Wise Evaluation and Comparison of White Matter Fiber Strain and Maximum Principal Strain in Sports-Related Concussion. *Journal of Neurotrauma*, 2015, 32: 441-454.
- [15] Mizuno K, Iwata K, Deguchi T, Ikami T, Kubota M. Development of a three-year-old child FE model. *Traffic Injury Prevention*, 2005, 6(4): 361–371.
- [16] Dong L, Li G, Mao H, Marek S, Yang K. Development and validation of a 10-year-old child ligamentous cervical spine finite element model. *Annals of Biomedical Engineering*, 2013, 41(12): 2538–2552.
- [17] Roth S, Raul JS, Willinger R. Biofidelic child head FE model to simulate real world trauma. *Computer Methods and Programs in Biomedicine*, 2008, 90: 262–274.
- [18] Li Z, Han X, Ge H, Ma C. A semi-automatic method of generating subject-specific pediatric head finite element models for impact dynamic responses to head injury. *Journal of the Mechanical Behavior of Biomedical Materials*, 2016, 60: 557-567.
- [19] Zhou Z, Jiang B, Zhu F, Mao H, Yang K. Numerical simulations of the 10-year-old head response in drop impacts and compression tests. *Computer Methods and Programs in Biomedicine*, 2016, 131: 13-25.
- [20] Burdi A, Huelke D, Snyder R, Lowrey G. Infants and children in the adult world of automobile safety design: pediatric and anatomical considerations for design of child restraints. *J. Biomech.* 2 (1969) 267–280.
- [21] Margulies S, Coats B. Experimental Injury Biomechanics of the Pediatric Head and Brain, in *Pediatric Injury Biomechanics*, 157-189, Springer, New York, USA, 2013.
- [22] Prange M, Margulies S. Regional, directional, and age-dependent properties of brain undergoing large deformation. *Journal of Biomechanical Engineering*, 2002, 124: 244–252.
- [23] Prange M, Luck J et al. Mechanical properties and anthropometry of the human infant head. *Stapp Car Crash Journal*, 2004, 48: 279–299.
- [24] Coats B, Margulies S. Material properties of human infant skull and suture at high rates. *Journal of Neurotrauma*, 2006, 23: 1222–1232.
- [25] Epstein HT. Correlated brain and intelligence development in humans. In *Development and evolution of brain size: Behavioral implications*, 111–131, M. E. Hahn, C. Jensen, & B. C. Dudek Editions, New York, USA, 1979.
- [26] Wilke M, Krageloh-Mann I et al. Global and local development of gray and white matter volume in normal children and adolescents. *Experimental Brain Research*, 2006, 178: 296–307.
- [27] Lenroot R, Gogtay N et al. Sexual dimorphism of brain developmental trajectories during childhood and

adolescence. *Neuroimage*, 2007, 36: 1065–1073.

- [28] Gooding C. Cranial sutures and fontanelles. In *Radiology of the Skull and Brain Vol.I, The Skull*, 216-240, Editors TH Newto, DJ Pots, The C.V. Mosby Company, St. Louis, MO, 1971.
- [29] Scheuer L, Black S. The juvenile skeleton. Elsevier Academic Press, San Diego, CA, 2004.
- [30] Jolivet E, Lafon Y, Petit P, Beillas P. Comparison of Kriging and Moving Least Square Methods to Change the Geometry of Human Body Models. *Stapp Car Crash Journal*, 2005, 59: 337-357.
- [31] Crandall J, Myers B, Meaney D, Schmidtke S. *Pediatric Injury Biomechanics*, Springer, New York, USA, 2013.
- [32] Matsuzawa J, Matsui M et al. Age-related Volumetric Changes of Brain Gray and White Matter in Healthy Infants and Children. *Cerebral Cortex*, 2001, 11:335-342.
- [33] Snyder RG, Schneider LW, Owings CL, Reynolds HM, Golomb DH, Sckork MA. Anthropometry of Infants, Children, and Youths to Age 18 for Product Safety Design. Internet: [<https://deepblue.lib.umich.edu/handle/2027.42/684>], 1977.
- [34] Li Z, Park BK et al. A statistical skull geometry model for children 0-3 years old, *PLoS One*, 2015, 10(5):e0127322.
- [35] Gefen A, Gefen N, Zhu Q, Raghupathi R, Margulies S. Age-Dependent Changes in Material Properties of the Brain and Braincase of the Rat. *Journal of Neurotrauma*, 2003, 20(11): 1163-1177.
- [36] Chatelin S, Vappou J, Roth S, Raul JS, Willinger R. Towards child versus adult brain mechanical properties. *Journal of Mechanical Behavior of Biomedical Materials*, 2012, 6: 166-173.
- [37] Kriewall TJ, Akkas N et al. Mechanical behavior of fetal dura mater under large asymmetric inflation. *Journal of Biomechanical Engineering*, 1983, 105: 71-76.
- [38] Bylski DI, Kriewall TJ et al. Mechanical behavior of fetal dura mater under large deformation biaxial tension. *Journal of Biomechanics*, 1986, 19: 19-26.
- [39] Jin X, Lee J et al. Biomechanical response of the bovine pia-arachnoid complex to tensile loading at varying strain-rates. *Stapp Car Crash Journal*, 2006, 50: 637–649.
- [40] Jin X, Ma C et al. Biomechanical response of the bovine pia-arachnoid complex to normal traction loading at varying strain rates. *Stapp Car Crash Journal*, 2007, 51: 115–125.
- [41] Bloomfield I, Johnston I et al. Effects of proteins, blood cells, and glucose on the viscosity of cerebrospinal fluid. *Pediatric Neurosurgery*, 1998, 28: 246–251.
- [42] McPherson G, Kriewall T. The elastic modulus of fetal cranial bone: a first step toward understanding of the biomechanics of fetal head molding. *Journal of Biomechanics*, 1980, 13: 9–16.
- [43] Margulies S, Thibault KL. Infant skull and suture properties: measurements and implications for mechanisms of pediatric brain injury. *Journal of Biomechanical Engineering*, 2000, 122: 364–371.
- [44] Davis MT, Loyd AM, Shen HH, Mulroy MH, Nightingale RW, Myers BS, Bass CD. The mechanical and morphological properties of 6 year-old cranial bone. *Journal of Biomechanics*, 2012, 45: 2493-2498.
- [45] Irwin A, Mertz H. Biomechanical bases for the crabi and hybrid III child dummies. *Proceeding of the 41th Stapp Car Crash Conference*, 1997, Lake Buena Vista, FL, USA.
- [46] Crichton ML, Donose BC, Chen X, Raphael AP, Huang H, Kendall MAF. The viscoelastic, hyperelastic and scale dependent behaviour of freshly excised individual skin layers. *Biomaterials* 32, 2011, 4670–4681.
- [47] Barkovich A, Kjos B et al. Normal maturation of the neonatal and infant brain: MR imaging at 1.5 T, *Radiology*, 1988, 166: 173–180.
- [48] Loyd AM. Studies of the Human Head From Neonate to Adult: An Inertial, Geometrical and Structural Analysis with Comparisons to the ATD Head. Dissertation. Department of Biomedical Engineering, Duke University, 2011.
- [49] Donnelly BR, Morgan RM, Eppinger RH. Durability, repeatability and reproducibility of the NHTSA side impact dummy. *Proceedings of the 27th Stapp Car Crash Conference*, 1983, San Diego, CA, USA.
- [50] Lange R.de, Rooij L.van, Mooi H, Wismans J. Objective biofidelity rating of a numerical human occupant model in frontal to lateral impact. *Stapp Car Crash Journal*, 2005, 49: 457-479.
- [51] Eppinger R, Sun E, Bandak F, Haffner M, Khaewpong N, Maltese M. Development of Improved Injury Criteria for the Assessment of Advanced Automotive Restraint Systems – II, NHTSA Report, 1999.

VIII. APPENDIX A

The NISE method was developed to evaluate the difference in acceleration responses obtained from side impact dummies [49]. It provides a means of comparing the differences in amplitude, phase and shape between two time history responses. The NISE for phase is calculated according to

$$NISE_{phase} = \frac{2R_{xy}(\tau)\max - 2R_{xy}(0)}{R_{xx}(0) + R_{yy}(0)} \quad (A1)$$

where

$$\begin{aligned} R_{xy}(\tau) &= \frac{1}{N-n} \sum_{i=1}^{N-n} X_i Y_{i+n} & R_{xy}(0) &= \frac{1}{N} \sum_{i=1}^{N-n} X_i Y_i \\ R_{xx}(0) &= \frac{1}{N} \sum_{i=1}^{N-n} X_i X_i & R_{yy}(0) &= \frac{1}{N} \sum_{i=1}^{N-n} Y_i Y_i \end{aligned} \quad (A2)$$

$$n = \frac{\tau}{\Delta t}$$

with X_i representing the i -th point of a data set (for example the experimental data) and Y_i representing the i -th point of the other data set (for example the simulated data). N is the number of discretised point in the data set and τ the time lag.

The NISE for amplitude is calculated after the phase shift has been eliminated. The expression for $NISE_{amplitude}$ is the following:

$$NISE_{amplitude} = \frac{R_{xy}(\tau)\max}{\sqrt{R_{xx}(0)R_{yy}(0)}} - \frac{2R_{xy}(0)\max}{R_{xx}(0) + R_{yy}(0)} \quad (A3)$$

The NISE for shape is also calculated after the phase shift has been eliminated according to

$$NISE_{shape} = 1 - \frac{R_{xy}(\tau)\max}{\sqrt{R_{xx}(0)R_{yy}(0)}} \quad (A4)$$

The Error Measures (EMs) estimated by the NISE method were used to calculate a Correlation Score (CS) as below

$$\begin{aligned} CS_{shape} &= 100 \times (1 - |NISE_{shape}|) \\ CS_{amplitude} &= 100 \times (1 - |NISE_{amplitude}|) \\ CS_{phase} &= 100 \times (1 - |NISE_{phase}|) \end{aligned} \quad (A5)$$